JOURNAL OF SOLID STATE CHEMISTRY **127,** 72–81 (1996)
ARTICLE NO. 0358

Infrared and Raman Spectra of $LiNH_3OHSO_4$ and $(NH_3OH)_2SO_4$ Single Crystals and Their Deuterated Analogs

V. P. Mahadevan Pillai* and V. U. Nayar†,[1]

*Department of Physics, St. Gregorious College, Kottarakara 691531, Kerala, India; and †Department of Optoelectronics, University of Kerala, Kariavattom, Trivandrum 695581, Kerala, India

Received April 1, 1996; in revised form August 13, 1996; accepted August 14, 1996

Infrared and Raman spectra of $LiNH_3OHSO_4$ and $(NH_3OH)_2SO_4$ single crystals and their deuterated analogs are recorded and analyzed. Bands are assigned on the basis of SO_4^{2-}, NH_3, and OH vibrations. The appearance of the ν_1 mode in the B_g species contributing to α_{xz}, α_{yz}, and α_{xy} polarizability tensor components, the higher wavenumber values of the ν_1 mode, the observation of the inactive ν_1 and ν_2 modes in the infrared spectrum, and the lifting of degeneracies of the ν_2, ν_3, and ν_4 modes suggest that the SO_4 tetrahedron in $LiNH_3OHSO_4$ is distorted confirming the X-ray data. The large splitting observed for the ν_1 mode in $(NH_3OH)_2SO_4$ and its decrease on deuteration indicate that the SO_4 tetrahedron is more distorted in it. Strong hydrogen bonds are formed between the H atoms of the NH_3 and OH groups with the oxygen atoms of the SO_4 group in both the crystals. The presence of two bands for the nondegenerate symmetric bending mode (ν_2), the broadness of the stretching modes ν_1 and ν_3 of NH_3, and the appearance of two NH_3 torsional bands at 90 K suggest the existence of two distinct $HONH_3^+$ sites in the $(NH_3OH)_2SO_4$ crystal confirming the inelastic neutron scattering data. The two NH_3 torsional modes observed at 90 K suggest that hydrogen bonds formed by NH_3 protons become more pronounced at low temperature. In $LiNH_3OHSO_4$ only one NH_3 torsional mode is obtained and this indicates that NH_3OH^+ sites in it are identical. ABC bands are observed in the OH stretching region in both of the crystals confirming the presence of strong hydrogen bonds. © 1996 Academic Press, Inc.

INTRODUCTION

$LiNH_3OHSO_4$ crystallizes in the orthorhombic system with space group *Pbca* and has eight formula units per unit cell (1). It has a structure which is quite different from the stuffed tetrahedral framework structures of the isoelectronic $Li(N_2H_5)SO_4$ and $Li(N_2H_5)BeF_4$ or the other compounds of the forms $LiMSO_4$ and $LiMBeF_4$ (M = K, Rb, Cs, and NH_4). $LiNH_3OHSO_4$ contains sheets of $LiSO_4$, hydrogen bonded together by the NH_3OH^+ ions. The Li atom is surrounded by four oxygen atoms at 1.96 Å and S by four oxygen atoms at 1.477 Å.

$(NH_3OH)_2SO_4$ crystallizes in the monoclinic system with space group $P2_1/c$ having four molecular units per unit cell (2). Detailed structure of this compound with bond lengths and bond angles is not available. There are only a few reports of the vibrational analysis of the compounds containing NH_3OH^+ ions (3–5). A detailed analysis of the vibrational spectra of $(NH_3OH)_2SO_4$, $(ND_3OD)_2SO_4$, $LiNH_3OHSO_4$, and $LiND_3ODSO_4$ has been carried out to obtain more information about the internal structure of these compounds and the nature of hydrogen bonding.

EXPERIMENTAL

Single crystals of $LiNH_3OHSO_4$ (abbreviated as LNHS) were prepared by the slow evaporation of the aqueous solution containing stoichiometric quantities of $(NH_3OH)_2SO_4$ and Li_2SO_4 at room temperature (300 ± 3 K). Single crystals of $(NH_3OH)_2SO_4$ (abbreviated as NHS) were prepared by the slow evaporation of the aqueous solution of commercially available $(NH_3OH)_2SO_4$ (BDH, AR grade) at room temperature. The deuterated analogs of these compounds were prepared by dissolving them in heavy water (99.99% pure) and evaporating the solution under a vacuum desiccator. The process was repeated several times to enhance the percentage of deuteration.

Well grown single crystals of LNHS and NHS were chosen and crystallographic axes were determined using a polarizing microscope. The sides x, y, and z of the crystals were chosen in accordance with crystallographic a, b, and c axes. The sides of the crystals were cut, finely polished, and properly aligned on the goniometer to record the Raman spectra in the 90° scattering geometry. The polarized Raman spectra of LNHS (Figs. 1–3) were recorded on six crystal orientations, viz., $y(xx)z$, $x(yy)z$, $x(zz)y$, $y(xy)z$, and $y(zy)z$. Polarized Raman spectra (Figs. 4 and 5) of NHS were recorded on four crystal geometries, viz., $z(yy)x$, $z(xz)x$, $z(yz)x$, and $z(xy)z$. Raman spectra of the polycrystalline samples of $LiNH_3OHSO_4$, $LiND_3ODSO_4$,

[1] To whom correspondence should be addressed.

0022-4596/96 $18.00

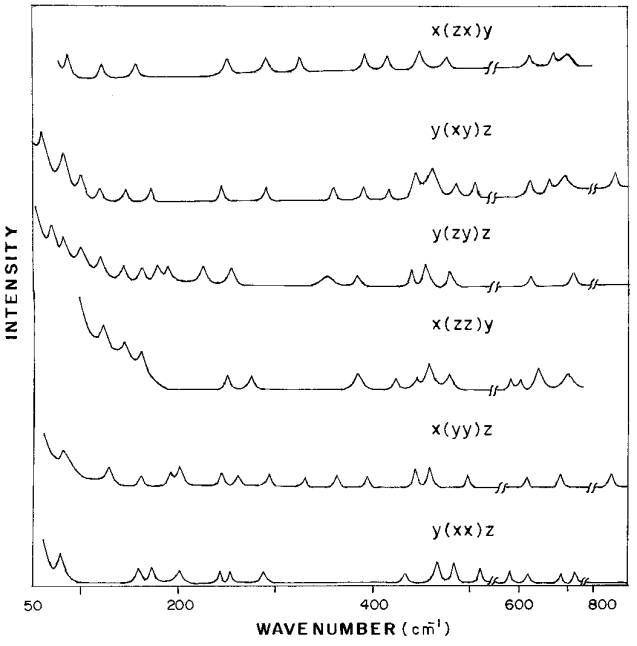

FIG. 1. Raman spectra of $LiNH_3OHSO_4$ in the 50–850 cm^{-1} region for $y(xx)z$, $x(yy)z$, $x(zz)y$, $y(zy)z$, $y(xy)z$, and $x(zx)y$ orientations.

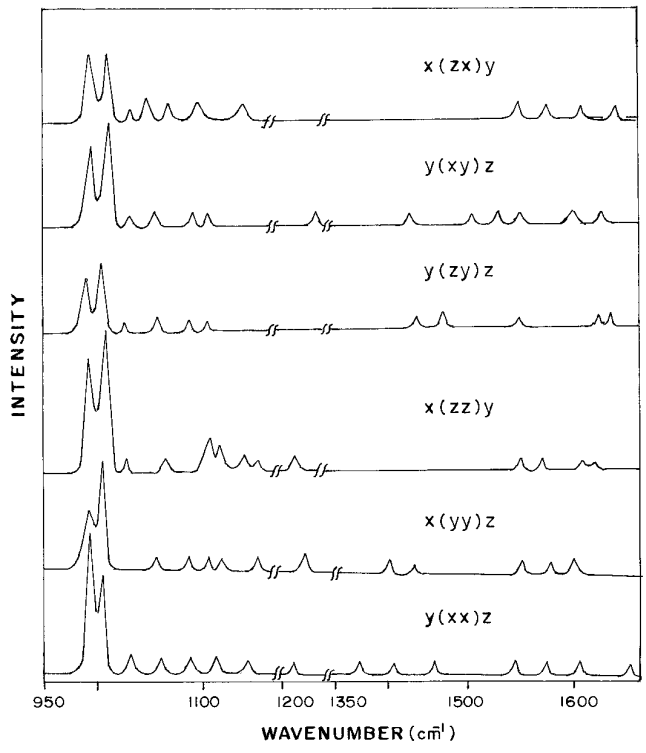

FIG. 2. Raman spectra of $LiNH_3OHSO_4$ in the 950–1650 cm^{-1} region for $y(xx)z$, $x(yy)z$, $x(zz)y$, $y(zy)z$, $y(xy)z$, and $x(zx)y$ orientations.

$(NH_3OH)_2SO_4$, and $(ND_3OD)_2SO_4$ were also recorded by taking the samples in capillary tubes. A 1401 Spex Raman spectrometer equipped with a Spectra Physics model 165.08 Ar^+ laser was used for recording Raman spectra. The spectra were recorded using 514.5 nm exciting radiation at a resolution better than 3 cm^{-1}. The Raman spectra of LNHS and NHS single crystals were recorded in the back scattering geometry, $x(z\ z + y)x$ and $x(y\ y + z)x$ geometries, respectively, at 300 and 90 K, using a Coherent Innova 300 krypton ion laser (exciting radiation 476.2 nm) and Raman spectra of NHS on a Dilor Z24 Raman spectrometer. The FTIR/IR spectra of LNHS, LNDS, NHS, and a partially deuterated $(ND_3OD)_2SO_4$ (abbreviated NDS) were recorded on a Bruker IFS-66V-FTIR spectrometer/Perkin–Elmer 882 spectrophotometer as polyethylene pellets and KBr pellets. Raman spectra are redrawn conforming to the original spectra obtained for the crystals and are given in Figs. 1–5.

FACTOR GROUP ANALYSIS

Li, NH_3OH^+, and SO_4^{2-} ions in LNHS and NH_3OH^+ and SO_4^{2-} ions in NHS occupy the general site C_1 in the respective crystals. Factor group analysis of the compounds has been carried out using the correlation method developed by Fateley *et al.* (6) (see Tables 1 and 2). The 285 irreducible representations obtained for LNHS excluding acoustic modes at $k = 0$ are distributed as

$$\Gamma_{LNHS} = 36A_g + 36B_{1g} + 36B_{2g} + 36B_{3g} + 36A_u + 35B_{1u} + 35B_{2u} + 35B_{3u}.$$

For NHS, 201 optical modes (at $k = 0$) are obtained. They are distributed as

$$\Gamma_{NHS} = 51A_g + 51B_g + 50A_u + 49B_u.$$

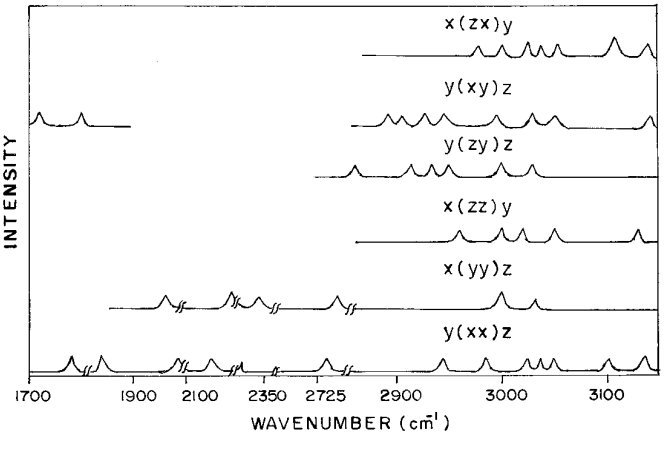

FIG. 3. Raman spectra of $LiNH_3OHSO_4$ in the 1700–3150 cm^{-1} region for $y(xx)z$, $x(yy)z$, $x(zz)y$, $y(zy)z$, $y(xy)z$, and $x(zx)y$ orientations.

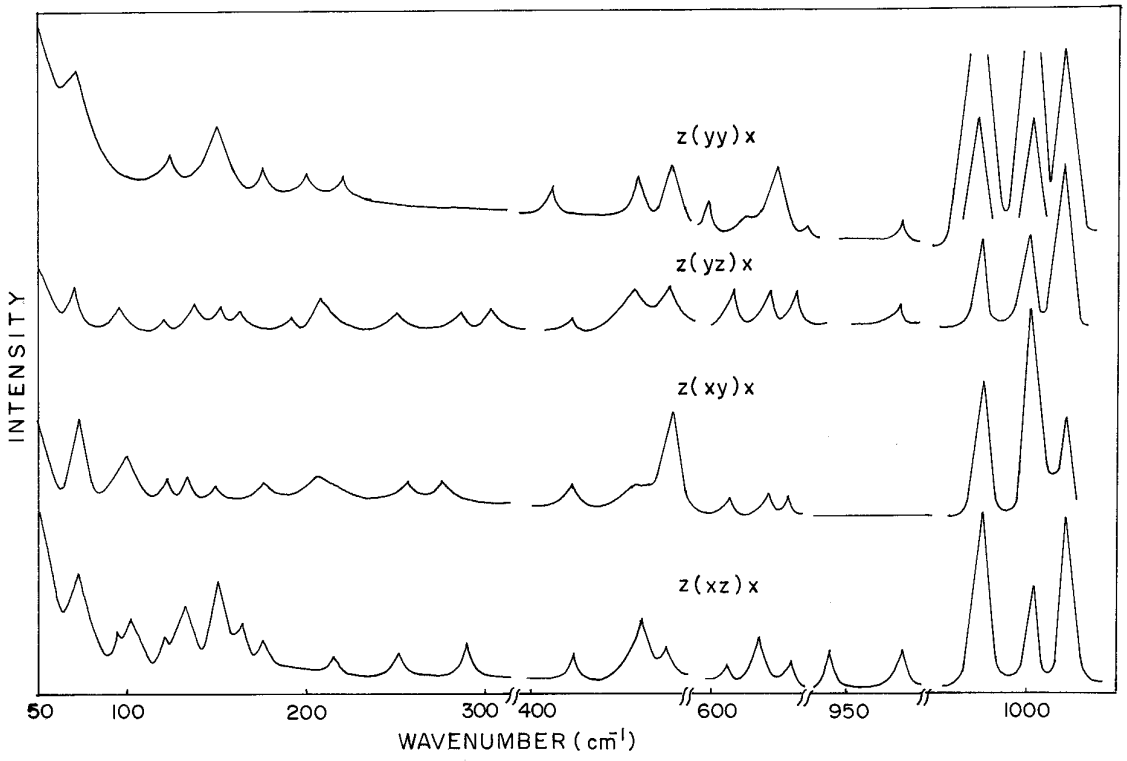

FIG. 4. Raman spectra of $(NH_3OH)_2SO_4$ in the 50–1050 cm^{-1} region for $z(xz)x$, $z(xy)x$, $z(yz)x$, and $z(yy)x$ orientations.

RESULTS AND DISCUSSION

SO_4^{2-} Vibrations

A free SO_4^{2-} ion under T_d symmetry has four fundamental vibrations, viz., the nondegenerate symmetric stretching mode $\nu_1(A_1)$, the doubly degenerate bending mode $\nu_2(E)$, the triply degenerate asymmetric stretching mode $\nu_3(F_2)$, and triply degenerate asymmetric bending mode $\nu_4(F_2)$. All the modes are Raman active, whereas only ν_3 and ν_4 are active in the IR.

$LiNH_3OHSO_4$ and $LiND_3ODSO_4$

The nondegenerate stretching mode of SO_4^{2-} (ν_1) splits into two in the Raman spectra in all the crystal orientations and in the back scattered spectrum for LNHS (Table 3). In $y(xx)z$ and $x(zz)y$ polarizations, two intense bands at 996 and 1011 cm^{-1} are obtained. In all other crystal orientations, these bands have only medium intensity. In $y(xx)z$ and $y(xz)x$ orientations, the band at 996 cm^{-1} shows more intensity than the band at 1011 cm^{-1}. However, in all other orientations, the band at 1011 cm^{-1} is more intense than the other band. In the back scattered Raman spectrum, two very intense bands are observed at 996 and 1010 cm^{-1}, with the band at 1010 cm^{-1} showing enhanced intensity. In the FTIR spectrum, an intense band is observed at 1001 cm^{-1} for this vibration. In the deuterated compound LNDS, two very intense bands are observed at 999 and 1009 cm^{-1} in the Raman spectrum and two weak bands at 980 and 1000 cm^{-1} in the IR spectrum.

The asymmetric stretching mode ν_3 of SO_4^{2-} is observed with degeneracy lifted in the Raman spectra in all the crystal orientations and in the back scattered spectrum (Table 3). In the FTIR spectrum, a very intense band is observed at 1132 cm^{-1} for this mode. In the deuterated compound, degeneracy is lifted in both the IR and Raman spectra.

The ν_2 mode of SO_4^{2-} appears with degeneracy lifted in the Raman spectra in all the crystal orientations. However, in the back scattered Raman spectrum and in the FTIR spectrum only a single band is observed. The asymmetric bending mode ν_4 also appears with degeneracy lifted in the Raman spectra, whereas it is partially retained in the FTIR spectrum.

Under T_d symmetry, the ν_1 mode has polarizability components α_{xx}, α_{yy}, and α_{zz} and it is expected to appear in the A_g orientations without any distortion of the SO_4 tetrahedra. This mode is also observed in B_{1g}, B_{2g}, and B_{3g} orientations with considerable intensity. Since the SO_4^{2-} ion occupies a site C_1, it can be seen from the correlation table that this mode can be active in the B_{1g}, B_{2g}, and B_{3g} species, due to the distortion of SO_4 tetrahedra from T_d

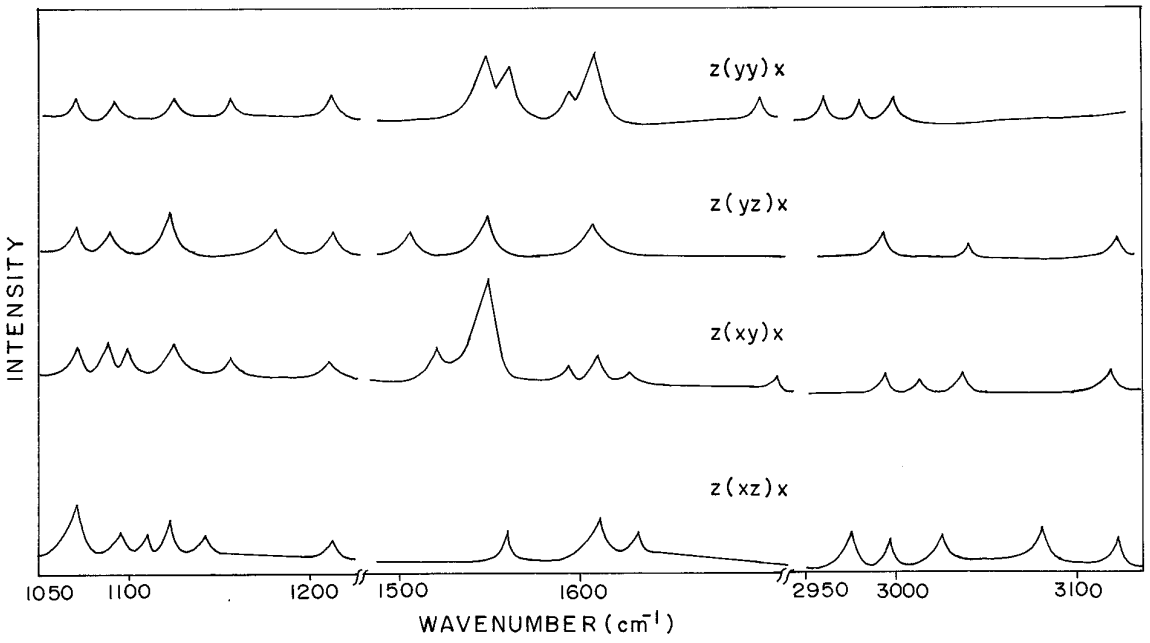

FIG. 5. Raman spectra of $(NH_3OH)_2SO_4$ in the 1050–3150 cm^{-1} region for $z(xz)x$, $z(xy)x$, $z(yz)x$, and $z(yy)x$ orientations.

to C_1, contributing to α_{xz}, α_{yz}, and α_{xy} polarizability tensor components (7). Higher wavenumber values obtained for the nondegenerate stretching mode ν_1 than those in a free SO_4^{2-} ion (8) also confirms the distortion of SO_4 tetrahedra as is evident from different S–O bond lengths determined from the X-ray diffraction studies (1, 9). Distortion of the SO_4^{2-} ion and the fact that there are eight molecular units in the Bravais cell leads to a splitting of the ν_1 mode and additional splitting, apart from the lifting of degeneracies of the ν_2, ν_3, and ν_4 modes. X-ray data show that H atoms of the NH_3 group and OH group form strong hydrogen bonds with the oxygen atoms of the SO_4 group with the N–H $\cdots$ O distance ranging from 2.799 to 3.066 Å and the O–H $\cdots$ O distance 2.65 Å. The presence of these hydrogen bonds may be the reason for the observed distortion in the SO_4 tetrahedra in LNHS. Deuteration does not affect the SO_4^{2-} vibrations.

$(NH_3OH)_2SO_4$ and $(ND_3OD)_2SO_4$

The nondegenerate symmetric stretching mode of the SO_4^{2-} ion exhibits larger splitting in both the FTIR and Raman spectra of NHS. Three very intense bands around 981, 1005, and 1021 cm^{-1} are obtained for this mode in $z(yy)x$ polarization of the Raman spectra of the crystal and in the powder spectrum (Table 4). Intensity of these bands alternates in the other polarizations. In the FTIR spectrum, only two intense bands at 978 and 1012 cm^{-1} are obtained. In the deuterated sample, three bands are again obtained but at 984, 992, and 1002 cm^{-1} in the Raman spectrum. In the FTIR spectrum of NDS, two intense bands are observed at 977 and 995 cm^{-1} for this mode. In NHS, the ν_1 mode has a frequency spread of 40 cm^{-1} in Raman and 34 cm^{-1} in the IR, while in NDS, this is only 18 cm^{-1} in both the spectra. This large splitting observed for the ν_1 mode in NHS and its decrease in NDS indicate that the SO_4 tetrahedron is distorted in NHS. Hydrogen atoms of NH_3 and OH groups form hydrogen bonds in the NHS crystal. Deuteration of the compound causes a reduction of the hydrogen bond strength, leading to a decrease in the spread of the splitting of this mode.

The degeneracies of the ν_2, ν_3, and ν_4 modes are lifted in the Raman spectra of the NHS crystal and of the dueterated compounds (Table 4). This can be expected from the lowering of the symmetry of the SO_4^{2-} ion from T_d to C_1. The appearance of the ν_1 mode in the B_g species also confirms the distortion of the SO_4 tetrahedra (7). The observed large splitting of the ν_1 mode in NHS compared to LNHS suggests that the SO_4^{2-} ion is more distorted in NHS.

NH_3OH^+ Vibrations

NH_3OH^+ vibrations consist of NH_3 and OH vibrations. NH_3 in the free state has C_{3v} symmetry and it has four fundamental vibrations, all being both Raman and IR active. The symmetric $[\nu_1(A_1)]$ and asymmetric $[\nu_3(E)]$ N–H stretching modes appear with weak intensity in the Raman spectra of all the compounds. In the FTIR spectrum of NHS, a very intense broad band is observed around 2955 cm^{-1} for both the stretching modes. Deuteration of this compound is only partial (about 70%) as seen from the stretching bands of ND_3 in NDS. These modes shift to

TABLE 1
Correlation of the Internal Vibrational Modes of SO_4^{2-} and NH_3 in $LiNH_3OHSO_4$

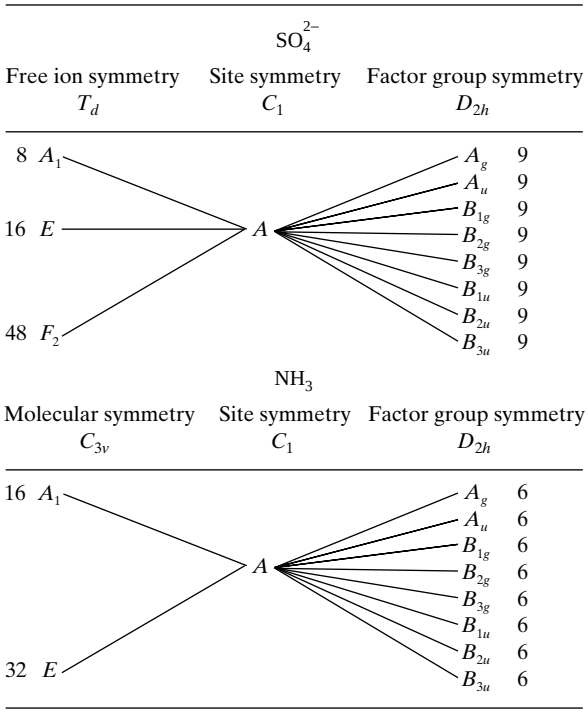

2267 cm^{-1} with shoulders at 2150 and 2375 cm^{-1} in the FTIR spectrum of the deuterated compound. In the Raman spectrum, they exhibit weak bands at 2155 and 2260 cm^{-1}. In the FTIR spectrum of LNHS, these modes obtained as an intense broad band around 2930 cm^{-1} are observed as two bands at 2285 and 2318 cm^{-1}.

The Raman bands appearing in the 1500–1650 cm^{-1} region in both NHS and LNHS are assigned to the bending modes ν_2 and ν_4 of NH_3. One intense band each is observed for ν_2 and ν_4 modes in the IR spectra for both LNHS and its deuterated analog. But in NHS, the nondegenerate ν_2 (NH_3) mode splits into two bands of equal intensity in both FTIR and Raman spectra while the degeneracy of the ν_4 mode is lifted in all the Raman orientations and in the FTIR spectrum.

From a study of the inelastic neutron scattering spectra, Jayasooriya *et al.* (5) predicted the existence of at least two distinct $HONH_3^+$ sites in the NHS crystal from two NH_3 torsional vibrations about the N–O axis. They have also obtained two IR NH_3 torsional modes at liquid nitrogen temperature. In the present study, the band at 416 cm^{-1} observed in the FTIR spectrum at room temperature is assigned to this mode as it disappears on deuteration. Weak bands are also observed in this region in the $z(yy)x$, $z(xz)x$, and $z(xy)x$ polarizations of the Raman spectra. Even though only one band is observed at room temperature for the torsional mode, the appearance of two bands in ν_2NH_3 mode region and the broadness of the ν_1 and ν_3 stretching modes can be considered as a confirmation of the existence of two distinct $HONH_3^+$ sites in the NHS crystal. Two bands are also obtained in NDS for the ν_2 mode with a higher wavenumber band at 1427 cm^{-1} having a higher intensity than the other (1387 cm^{-1}).

The N–H stretching frequencies ν_1 and ν_3 appear at lower wavenumbers than those in a free NH_3 group (8, 10) indicating that strong hydrogen bonds are formed by the H atom of the NH_3 group with the oxygen atoms of the SO_4^{2-} anion in both LNHS and NHS crystals. This is consistent with the X-ray structural data of N–H $\cdots$ O distances of 2.799–3.066 Å obtained for LNHS (1).

Two weak bands are observed at 2000 and 2059 cm^{-1} in the FTIR spectra of NHS. They are assigned to combination bands of the NH_3 deformations (1614 cm^{-1}) and NH_3 torsional modes (380 and 430 cm^{-1}). Similar combination bands have been observed earlier in $N_2H_6SO_4$ crystals (11). In LNHS, only one band around 1950 cm^{-1} is obtained in this region.

The positive isotope effect implies a weakening of the hydrogen bonds on deuteration (12, 13). The isotopic frequency ratios observed for the N–H stretching modes for NHS and LNHS are about 1.289 and 1.267, respectively. For the bending modes, these ratios have values of 1.10156 and 1.1868, respectively. For a free molecule, this ratio is about 1.355. This value decreases as the strength of the hydrogen bond increases. Therefore, the lower values obtained for this ratio also indicate the presence of strong hydrogen bonds in $LiNH_3OHSO_4$ and $(NH_3OH)_2SO_4$.

TABLE 2
Correlation of the Internal Vibrational Modes of SO_4^{2-} and NH_3 in $(NH_3OH)_2SO_4$

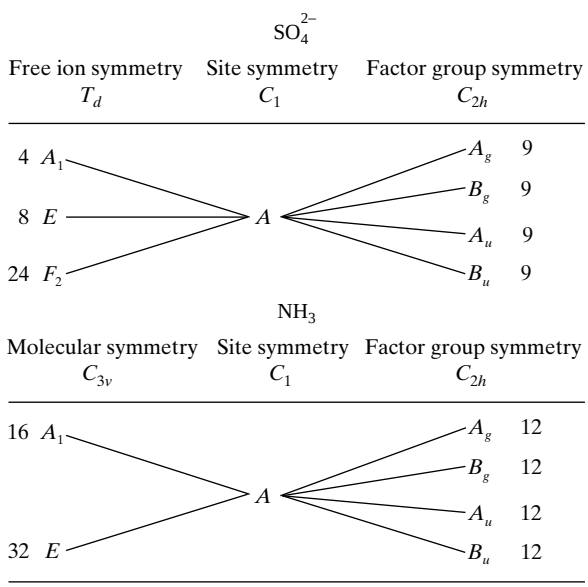

TABLE 3
Spectral Data (cm^{-1}) and Band Assignments for $LiNH_3OHSO_4$ and $LiND_3ODSO_4$

$LiNH_3OHSO_4$										$LiND_3ODSO_4$		
		Raman						Back scattered				
IR	FTIR	$y(xx)z$	$x(yy)z$	$x(zz)y$	$x(zx)y$	$y(xy)z$	$y(zy)z$	300 K	90 K	Raman	IR	Assignments
1	2	3	4	5	6	7	8	9	10	11	12	13
	63vw					56w	70w					
	87vs	77w	79w		88w	81m	81w		94w	80w		SO_4 translation
	102w		131w	120w	121w	101vw	101vw	116w	115w			
	131m					121w	121w			130w		$\delta(O \cdots O)$
	141vw			141w		146vw	141vw	145w	148w	140w		
									167vw			SO_4 libration
	150w	159w	165vw	161vw	161vw	166vw	161vw		207vw	174vw		
	169m	170vw	191w				176vw	230wbr	226vw	221w		NH_3OH translation
	198s	201w	201w				190vw					
	240sh	246w	246w	251w	250w	241vw	226vw	245vwbr	248vw			
		255vw	259w	266w			261w					
	286sbr	285w	290w		285vw	285w		290w		240w		$\nu(O \cdots O)$
	333vs		330vw		325w							
			365w			361vw	360vwbr		365w			Li^+ translation
390w	388vs		390w	386w	390w	391vw	381vw			380w	408w	Li–O stretch
	422vs	434vw	425vw	425vw	415vw	415vw			430m			NH_3 torsion
440w		463wbr	440w	445w	456w	449w	441vw	450m	452m	444m	468m	
472m	474vs	481w	455w	454m	481w	456w	451w		486m	450m	482w	ν_2SO_4
				481w		486vw	481w			461vw		
										476w		
520vw		505w	491w			505vw			503vw		519w	Li–N stretch
621s	600sh	585vw		591vw						610sh		
	639vs	615vw	615vw	601vw	615vw	615vw	615vw	618mbr	617m	625w	618s	ν_4SO_4
		643w	641vw	621m	638w	635vw	655w	635w	638w	635m	642sh	
		651w		651wbr	651w	646wbr		648m	647wbr	651w		
752w	800sh											γ(OH)
			820w							674w		NH_3/ND_3 rock
										890w		$2\nu_2SO_4$
										917vw		
995m	1001s	996s	996m	996s	996m	998m	997m	996vs	997s	996vs	980w	ν_1SO_4
		1011s	1010s	1011s	1011m	1010m	1011m	1010vs	1011vvs	1009vs	1000w	
		1030vw		1030w	1030w	1030w	1031vw	1038vw		774vw		N–OH/N–OD stretch
1083w		1061w	1061w	1066w	1046w	1056w	1068w	1083sh	1087m	1052vw	1050m	ν_3SO_4
1087vs		1086w	1086vw	1103m	1066w	1091w	1091vw	1102s	1102s	1065vw	1092vs	
1121vs	1132vsbr	1111w	1106w	1113w	1101w	1101w	1106vw	1138w	1143m	1117vw	1127vs	
		1145vw	1116vw	1140w	1143w			1153w	1157m	1141vw	1162s	
			1156w	1156w					1177w	1151vw		
1245mbr		1210vw	1220w	1210w		1206vw		1214w	1218mbr	922vw	923m	δOH/OD
										960vw	1032m	
1405vw		1375w										
		1405w	1430vw			1425vw	1430vw					Combinations
		1440w					1455w					
1525s	1506s	1540w	1556vw	1545w	1551w	1516vw	1550w	1516w	1521vw	1193m	1232m	ν_2NH_3/ND_3
1565s		1561w	1581w	1566w	1571w	1526vw		1535vw	1534vw	1275w		
		1580w				1548w						
1640s	1614s	1605vw	1600w	1616w	1611w	1600w	1625vw	1618mbr	1615w	1376w	1360w	
		1660w			1640w	1626w	1635vw		1624m	1430w	1422w	ν_4NH_3/ND_3
						1676vw						
	1760w	1746w								1615vw	2165w	
		1870w				1711w				1660vw		Combinations
		2125vw	2140w			1760vw						
1935wbr	1950w	1945w	1930w									NH_3 torsion–NH_3 deformation
2230vw	2365w	2330w	2340vw								1750w	ν(OH) A & B bands
2725m	2697vs	2730wbr	2740w							2060w	2060w	
									2804w			
									2832m			Combinations
									2859m			
2920m	2930sbr	2945w		2960w	2970w	2890w	2860w	2916w	2872w	2176w	2285s	
3030s		2985w	2995w	2995w	3020w	2905w	2915vw	2964w	2900w	2260s	2318m	
		3020w	3030w	3020w	3030w	2930vw	2935vw	3010w	2935s	2360sbr	2390m	ν_1 & ν_3 NH_3/ND_3
		3035w		3052w	3050w	2945w	2950vw	3050w	2954w	2990vw	2941vw	
		3050vw		3130w	3110w	2990w	3000vw		3012w	3014vw	3055vw	
		3100vw			3140vw	3030w	3030vw		3086w			
						3050w			3122w			
3140vw						3140w			3152w			Combinations
									3259w			

Note. vs, very strong; s, strong; m, medium; vw, very weak; w, weak; br, broad; sh, shoulder.

TABLE 4
Spectral Data (cm^{-1}) and Band Assignments

$(NH_3OH)_2SO_4$									
Raman									
				Back scattered			$(ND_3OD)_2SO_4$		
$z(yy)x$	$z(xz)x$	$z(yz)x$	$z(xy)x$	300 K	90 K	FTIR	FTIR	Raman	Assignments
1	2	3	4	5	6	7	8	9	10
							60vw		
72w	72m	72w	74m	80w	69m	87vs	69vw	85w	SO_4 translation
	92w	98w	96mbr	95vw	84w		87w		
	100w			107vw	96w				
124w	120vw	120vw	120vw		111vw	125s	125sh	126m	SO_4 libration
150m	130m	135w	130vw	139w	135m	150mbr		150w	$\delta(O \cdots O)$?
	152m	150w	145vw	158m	160w				
175vw	165sh	160w	170vw	175m	177m	190vsbr	190sh	195w	SO_4 libration
	175vw	192w			192vw				
200vwbr	215vw	205mbr	200wbr	212mbr	204m	230vs	218vs		NH_3OH translation
215w	250w	250w	255vw		217m		265sh		
					223vw				
				259w	259vw				
	285w	286w	270vw	288w	289m	290sh		274w	$\nu(O \cdots O)$
		300w			306w			295vw	
410w	420w		420w		380m				
					424m	417vs			NH_3 torsion
460w	458m	455m	455sh	454m	460m	459m	468s	456m	ν_2SO_4
475m	475w	475m	478s	475m	473m	471m		478m	
							577s		OD torsion?
595w	605w	610w	610vw	603w	601w	603vs	610vs	620w	
620sh	625m	630w	630w	626m	619m	615vs	635vs	643w	ν_4SO_4
637m	640vw	641w	638vw	638sh	627m	627vs			
					637m				
655vw					656vw				OH torsion
						831s	650sh	665vw	γOH/OD
							835w		
880vw	835w	880vw		842w	850m				NH_3 rocking
	880w								
981vs	981s	983m	981s	979vs	978vs	978s	977s	984vs	
1005vs	1003m	1004m	1004vs	1002s	999s	1012s	995s	992vs	ν_1SO_4
1021vs	1021s	1020s	1021s	1017vs	1017vs			1002vs	
1070w	1070m	1070w	1070vw	1067w	1067m	1066vs	1097vsbr	1075wbr	
1090w	1090w	1089vw	1085w	1084w	1086m	1120sh	1183sh	1110w	ν_3SO_4
1122vw	1110vw	1122m	1094w	1115w	1102w			1170w	
1160vw	1120w	1185w	1120w		1121m				
	1150w		1160vw						
1215w	1215w	1215w	1210wbr	1208wbr	1217mbr	1215s	892m	950w	δN–OH/N–OD
							931m		
1550m	1560vw	1505w	1520w	1506vw	1508w	1523s	1387m	1265vw	
1560w		1550w	1550m	1550w	1552w	1558s	1427m	1330m	
							1529m		ν_2NH_3/ND_3
							1557m		
1594w	1610w	1610wbr	1590vw	1608w	1583vw	1616s	1467m	1350w	
1608m	1635vw		1610w		1614m	1654sh	1616w	1390w	
1700vw			1625vw						ν_4NH_3/ND_3
			1713vw						
						2000w	1874vw		NH_3 deformation + NH_3
						2059w			torsion

TABLE 4—*Continued*

$(NH_3OH)_2SO_4$									
Raman									
				Back scattered			$(ND_3OD)_2SO_4$		
$z(yy)x$	$z(xz)x$	$z(yz)x$	$z(xy)x$	300 K	90 K	FTIR	FTIR	Raman	Assignments
1	2	3	4	5	6	7	8	9	10
						2100w			Combinations
						2230w			
						1684sh			
						2400sh	1765w		
				2737wbr	2710vw	2739vs	2055w		ν(OH) ABC bands
					2750vw		2793m		
2960w	2975w	2990w	2990w	2963m	2911vw	2955vs	2150sh	2115w	
2980w	2990w				2928w		2887s	2145w	ν_1NH_3/ND_3
								2155w	
2999w	3030w		3015vw	3011m	3019w		2267vs	2260w	
	3080w		3040vw	3122m	3032w		2375sh		
	3120vw	3120vw	3120vw		3063vw				ν_3NH_3/ND_3
				3200w	3129w				

Three fundamental vibrations connected with the hydrogen bonded OH groups are ν(OH) stretching and inplane δ(OH) and out-of-plane γ(OH) bending vibrations. In a strongly hydrogen bonded system, the νOH band is usually very broad due to strong interactions between the proton vibrations and the $\nu(O \cdots O)$ vibrations (14, 15). Due to Fermi resonance, the overtones of the δOH and γOH modes interact with the broad νOH band leading to the appearance of three bands A, B, and C in the νOH stretching region (16). In $LiNH_3OHSO_4$, strong hydrogen bonds are present between H atoms of the OH group of the NH_3OH^+ ion and O atoms of the SO_4 groups with $O \cdots O$ distances of around 2.65 Å. In NH_4HSeO_4, A, B, and C bands are obtained at 2655, 2290, and 1610 cm^{-1}, respectively, where the $(O \cdots O)$ distance is around 2.56 Å (17, 18). In $CsHSeO_4$, with $(O \cdots O)$ distances around 2.605 Å, they are observed at 2750, 2380, and 1600 cm^{-1}, respectively (19). In the IR and Raman spectra of the powder (20) samples of $LiNH_3OHSO_4$ and $LiND_3ODSO_4$ reported earlier, the bands at 3110, 2725, and 1935 cm^{-1} have been assigned to the ABC triplets, but in the FTIR spectrum no band is obtained around 3110 cm^{-1}. Therefore A, B, and C bands in the FTIR and Raman spectra are reassigned by considering the $O \cdots O$ distance (2.65 Å) in this crystal.

In the FTIR spectrum of LNHS, a broad intense band from 3150 to 2850 cm^{-1} with a peak at 2930 cm^{-1} is obtained. This broad band must be due to the symmetric and asymmetric N–H stretching modes as the H atoms in NH_3 group also form hydrogen bonds. Therefore the A and B bands are assigned at 2694 and 2363 cm^{-1}, respectively. The C band cannot be identified as it is masked by the NH_3 bending modes. In LNDS, the A and B bands shift to 2060 and 1750 cm^{-1} in the IR spectrum.

In $(NH_3OH)_2SO_4$, the A and B bands are not well resolved. A broad band extending from 2800 to 2200 cm^{-1} appears in the FTIR spectrum, with a peak at 2739 cm^{-1} and a shoulder at 2400 cm^{-1}. The C band is also observed as a shoulder at 1684 cm^{-1}. In the Raman spectrum, the A band is observed as a weak one at 2737 cm^{-1}. In the deuterated compound $(ND_3OD)_2SO_4$, the A and B bands are observed at 2055 and 1765 cm^{-1}, respectively. However, the C band is not identified as it is masked by the strong S–O stretching modes. The δ(OH) and γ(OH) modes are also assigned in both the LNHS and NHS (Tables 3 and 4).

The isotopic frequency ratio for A and B bands are of the order obtained for the NH_3 stretching modes indicating strong hydrogen bonds of the type $O–H \cdots O$ in the crystal. The $(O \cdots O)$ stretching mode is observed around 290 cm^{-1} is the Raman spectra of LNHS. On deuteration this band shifts to 240 cm^{-1}. This mode is obtained as a weak band around 288 cm^{-1} in the Raman spectra and as a shoulder around 290 cm^{-1} in the FTIR spectrum of NHS. A medium intense band is observed around 150 cm^{-1} in most of the crystal orientations of the Raman spectra of NHS. In the FTIR spectrum, a broad band is also obtained in this region. On deuteration the intensity of this band is considerably reduced. Hence, this band is assigned to the $\delta(O \cdots O)$ mode (15).

The –OH torsional modes occur at considerably higher

frequencies, owing to the shorter O–H bond and much lower moment of inertia compared to the NH_3 group. In the inelastic neutron scattering study, –OH torsional mode appears as a broad band around 656 cm^{-1} (5). In the FTIR spectrum of NHS, this mode is not identified as they are masked by the strong asymmetric bending vibration of SO_4^{2-}. However, in the deuterated compound a new mode is observed at 577 cm^{-1} and is assigned to the –OD torsional modes.

External Modes (*Lattice Modes*)

Lattice modes are observed below 400 cm^{-1}. An unambigous assignment of bands in this region is difficult as a large number of bands due to translational and rotational modes of anions and cations appears there. The translational mode of the Li^+ ion occurs at a higher wavenumber than those of other lattice modes in the 300–400 cm^{-1} region (21). These bands will not be observed in NHS. Therefore the bands observed around 365 cm^{-1} in a few crystal orientations of the Raman spectra are assigned to the translational modes of the Li^+ cation (22). The bands around 380 cm^{-1} are due to Li–O stretching modes (23, 24). These bands are not affected by deuteration. The Raman band around 87 cm^{-1} in NHS remains intact on deuteration. This suggests that these bands are due to the translational modes of SO_4^{2-} (25).

Temperature Effects

Back scattered Raman spectra of single crystals of $LiNH_3OHSO_4$ and $(NH_3OH)_2SO_4$ recorded at 300 and 90 K show significant variations.

$LiNH_3OHSO_4$. Two very intense bands are observed at 300 K around 995 and 1010 cm^{-1} in the ν_1 mode region of the SO_4^{2-} ion. At 90 K, the band at 995 cm^{-1} shifts to 997 cm^{-1} but with reduced intensity while the other band around 1011 cm^{-1} appears with an enhancement of the intensity. Both these bands become sharp at low temperature. In the asymmetric SO_4^{2-} stretching region the shoulder at 1083 cm^{-1} disappears and a medium intense band appears around 1087 cm^{-1} at 90 K. The intensity of the band at 1102 cm^{-1} is enhanced and the weak bands at 1138 and 1153 cm^{-1} are shifted to 1143 and 1157 cm^{-1} with enhanced intensity. A new band is also observed at 1177 cm^{-1}.

The single band at 450 cm^{-1} appearing for the ν_2 mode in the back scattered spectrum recorded at 300 K splits into two bands at 452 and 485 cm^{-1} in the low temperature spectra. In the ν_4 mode, intensity sharing of the bands is observed. In the room temperature spectra, the band at 617 cm^{-1} is broader and less intense than the bands at 648 cm^{-1}. At 90 K, the band at 618 cm^{-1} becomes sharper and gains intensity, while the band at 647 cm^{-1} becomes less intense but broad.

In the NH_3 stretching mode region bands at 90 K are shifted to lower wavenumbers indicating the strengthening of hydrogen bonds. Splitting of bands and considerable increase in intensity of bands are also observed. These indicate Fermi resonance between NH_3 stretching modes and the combinations and overtones of NH_3 deformation vibrations (26). This implies that hydrogen bonds become stronger at low temperature.

Torsional modes of NH_3, which were absent at the room temperature back scattered Raman spectra, appear at 430 cm^{-1} at 90 K. This band is assigned in comparison with the corresponding bands observed in NHS. As explained in the following section of NHS, the appearance of this band indicates the strengthening of hydrogen bonds in LNHS at 90 K.

$(NH_3OH)_2SO_4$. In the spectra recorded at room temperature, three bands are obtained for the ν_1 mode of SO_4^{2-}. The band at 979 cm^{-1} has a higher intensity than the band at 1017 cm^{-1}. At 90 K, the Raman band at 978 cm^{-1} has lesser intensity than the band at 1017 cm^{-1}. Thus intensity sharing takes place among the bands in NHS. In the ν_3 mode region, bands observed at 90 K are at higher wavenumbers and at larger intensity than those observed at 300 K. A new band is also observed at 1102 cm^{-1}. The sharing of intensity between bands for the ν_2 mode is also obtained in NHS. Moreover, the separation between the ν_2 bands reduces to 13 cm^{-1} at 90 K from 21 cm^{-1} at 300 K. In the asymmetric bending mode (ν_4) region the medium intense band at 626 cm^{-1} splits into two medium intense bands at 619 and 627 cm^{-1} and the shoulder at 638 cm^{-1} becomes well resolved to a band at 637 cm^{-1}.

As explained earlier, Jayasooriya *et al.* (5) observed two NH_3 modes at 380 and 425 cm^{-1} in the IR spectrum recorded at liquid nitrogen temperature. In the present study two medium intense bands are obtained at 380 and 424 cm^{-1} in the back scattered Raman spectrum at 90 K, confirming the observation of Jayasooriya *et al.* (5) of the existence of two distinct NH_3OH^+ sites in the crystal lattice. It may be noted that these bands are not observed in the back scattered Raman spectra at room temperature even though one band each is observed in certain polarizations of the Raman spectra. At low temperature, hydrogen bonds formed by the NH_3 protons become more pronounced and the distinct nature of two NH_3OH^+ sites becomes more clear leading to the appearance of two NH_3 torsional modes. This also confirms that the NH_3OH^+ sites in LNHS are identical since only one band is obtained for the NH_3 torsional mode.

Bands corresponding to the $\nu(O \cdots O)$ and $\delta(O \cdots O)$ modes appear at 90 K with enhanced intensity indicating the strengthening of hydrogen bonds.

In the Raman spectrum recorded at 90 K, the OH torsional mode is observed as a very weak broad band around 656 cm^{-1} and is immersed in the background of noise.

CONCLUSIONS

The appearance of the ν_1 mode in the B_g species contributing to α_{xz}, α_{yz}, and α_{xy} polarizability tensor components, the higher wavenumber values of the ν_1 mode, the observation of the inactive ν_1 and ν_2 modes in the infrared spectrum, and the lifting of degeneracies of the ν_2, ν_3, and ν_4 modes suggest that the SO_4 tetrahedron in LNHS is distorted confirming the X-ray data. The large splitting observed for the ν_1 mode in NHS and its decrease in NDS indicate that the SO_4 tetrahedron is more distorted in NHS. Strong hydrogen bonds are formed between the H atoms of the NH_3 and OH groups with the oxygen atoms of the SO_4 group in both LNHS and NHS crystals. The presence of two bands for the nondegenerate symmetric bending mode (ν_2), the broadness of the stretching modes ν_1 and ν_3 of NH_3, and the appearance of two NH_3 torsional bands at 90 K suggest the existence of two distinct $HONH_3^+$ sites in the NHS crystal confirming the inelastic neutron scattering data. The two NH_3 torsional modes observed at 90 K suggest that hydrogen bonds formed by NH_3 protons become more pronounced at low temperature. In LNHS only one NH_3 torsional mode is obtained and this indicates that NH_3OH^+ sites in it are identical. ABC bands are observed in the OH stretching region in both the crystals, confirming the presence of strong hydrogen bonds.

REFERENCES

1. S. Vilminot, M. R. Anderson, and I. D. Brown, *Acta Crystallogr. B* **29,** 2628 (1973).
2. S. Vilminot, L. Cot, C. Avinens, and M. Maurin, *Mater. Res. Bull.* **6,** 189 (1971).
3. D. L. Frasco and E. L. Wagner, *J. Chem. Phys.* **30,** 1124 (1959).
4. C. A. Van Dijk and R. G. Priest, *Combustion Flame* **57,** 15 (1984).
5. U. A. Jayasooriya, C. J. Ludman, C. I. Ratcliffe, and T. C. Waddington, *J. Chem. Soc. Faraday Trans. 2*, **77,** 287 (1981).
6. W. G. Fateley, F. R. Dollish, N. T. Mc Devitt, and F. F. Bentley, ''Infrared and Raman Selection Rules for Molecular and Lattice Vibrations—Correlation Method.'' Wiley–Interscience, New York, 1972.
7. R. Bhattacharjee, *J. Raman Spectrosc.* **21,** 491 (1990).
8. G. Herzberg, ''Molecular Spectra and Molecular Structure–Infrared and Raman Spectra of Polyatomic Molecules.'' Van Nostrand, New York, 1960.
9. F. D. Hardcastle and I. E. Wachs, *J. Raman Spectrosc.* **21,** 683 (1990).
10. K. Nakamoto, ''Infrared Spectra of Inorganic and Coordination Compounds.'' Wiley–Interscience, New York, 1970.
11. V. Varma and C. N. R. Rao, *J. Mol. Struct.* **268,** 1 (1992).
12. A. Novak, *in* ''Structure and Bonding'' (J. D. Dunitz, Ed.), Vol. 119, p. 176. Berlin Heidelberg, New York, 1973.
13. S. N. Vinogradov and R. H. Linnel, ''Hydrogen Bonding.'' Van Nostrand–Reinhold, New York, 1971.
14. S. Bratos and H. Rataczak, *J. Chem. Phys.* **76,** 77 (1982).
15. B. Marchon and A. Novak, *J. Chem. Phys.* **78,** 2105 (1983).
16. D. Hadzi and S. Bratos, *in* ''The Hydrogen Bond—Recent Theory and Experiments'' (P. Schuster, G. Zundel, and C. Sandorfy, Eds.), Vol. 2, p. 565. North-Holland, Amsterdam, 1976.
17. B. Pasquier, N. Le Calve, A. Rozycki, and A. Novak, *J. Raman Spectrosc.* **21,** 465 (1990).
18. Ph Colomban, M. Pham Thi, and A. Novak, *J. Mol. Struct.* **161,** 1 (1987).
19. J. Baran, *J. Mol. Struct.* **162,** 229 (1987).
20. V. P. Mahadevan Pillai, T. Pradeep, G. Suresh, and V. U. Nayar, *J. Raman Spectrosc.* **23,** 235 (1992).
21. R. Frech and E. Cazzanelli, *Solid State Ionics* **9/10,** 95 (1983).
22. S. H. Brown and R. Frech, *Spectrochim. Acta A* **44,** 1 (1988).
23. G. Sekar, G. Aruldhas, and V. Ramakrishnan, *J. Pure Appl. Phys.* **26,** 570 (1988).
24. J. Tarte, *J. Org. Nucl. Chem.* **29,** 915 (1969).
25. V. I. Torgashev, Yu I., Yuzyuk, L. M. Rabkin, and R. M. Feosyuk, *Sov. Phys. Crystallogr.* **33,** 82 (1988).
26. I. A. Oxten and O. Knop, *J. Mol. Struct.* **43,** 17 (1978).